

# International Conference on Space Optics—ICSO 2010

Rhodes Island, Greece

4–8 October 2010

*Edited by Errico Armandillo, Bruno Cugny,  
and Nikos Karafolas*



## ***Laser-induced contamination control for high-power lasers in space-based LIDAR missions***

*Jorge Alves, Federico Pettazzi, Adrian Tighe, Denny Wernham*



International Conference on Space Optics — ICSO 2010, edited by Errico Armandillo, Bruno Cugny,  
Nikos Karafolas, Proc. of SPIE Vol. 10565, 1056524 · © 2010 ESA and CNES  
CCC code: 0277-786X/17/\$18 · doi: 10.1117/12.2309274

# LASER-INDUCED CONTAMINATION CONTROL FOR HIGH-POWER LASERS IN SPACE-BASED LIDAR MISSIONS

Jorge Alves<sup>(1)</sup>, Federico Pettazzi<sup>(1)</sup>, Adrian Tighe<sup>(2)</sup>, Denny Wernham<sup>(3)</sup>

(1) *Opto-electronics Section*

(2) *Materials Space Evaluation & Radiation Effects Section*

(3) *ADM-Aeolus Project*

*European Space Agency ( ESTEC), Keplerlaan 1, 2200AG Noordwijk, The Netherlands*

## ABSTRACT

In the framework of the ADM-Aeolus satellite mission, successful test campaigns have been performed in ESTEC's laser laboratory, and the efficiency of several mitigation techniques against Laser-Induced Contamination (LIC) have been demonstrated for the ALADIN laser. These techniques include the standard contamination control methods of materials identification with particular tendency to cause LIC, reduction of the outgassing of organic materials by vacuum bake-out and shielding of optical surfaces from the contamination sources. Also novel mitigation methods such as in-situ cleaning via partial pressures, or the usage of molecular absorbers were demonstrated. In this context, a number of highly sensitive optical measurement techniques have been developed and tested to detect and monitor LIC deposits at nanometre level.

## 1. INTRODUCTION

The European Space Agency (ESA) is currently developing a novel measurement system to measure wind speeds and aerosol particle concentration in the troposphere and stratosphere from a space-borne instrument. ESA's project ADM-Aeolus has as its payload a LIDAR (Light Detection And Ranging ) system called ALADIN (Atmospheric Laser Doppler Instrument). The ALADIN laser is a diode-pumped Nd:YAG pulsed laser, generating pulses at the fundamental IR frequency (1064nm) which are subsequently frequency doubled (532nm) and tripled by non-linear crystals to produce the UV third harmonic (355nm) with an energy of around 100mJ at 100 Hz frequency. ALADIN will emit spectrally narrow UV laser pulses towards the atmosphere, directed at a 35° emission angle, probing the lowermost 30 km of wind profiles from an orbit 400 km above the Earth's surface.

## 2. BACKGROUND

Laser-Induced Contamination is a known phenomenon responsible for the degradation of the properties of optical components in vacuum [1] [2] [3]. Such degradation is due to the formation of a deposit in the optical surface area irradiated by the UV laser beam under vacuum (see Figure 1). The deposit growth is proposed to be the result of photochemical and photothermal mechanisms, which are triggered by the interaction between UV laser radiation and nearby outgassing species in vacuum from polymeric materials.

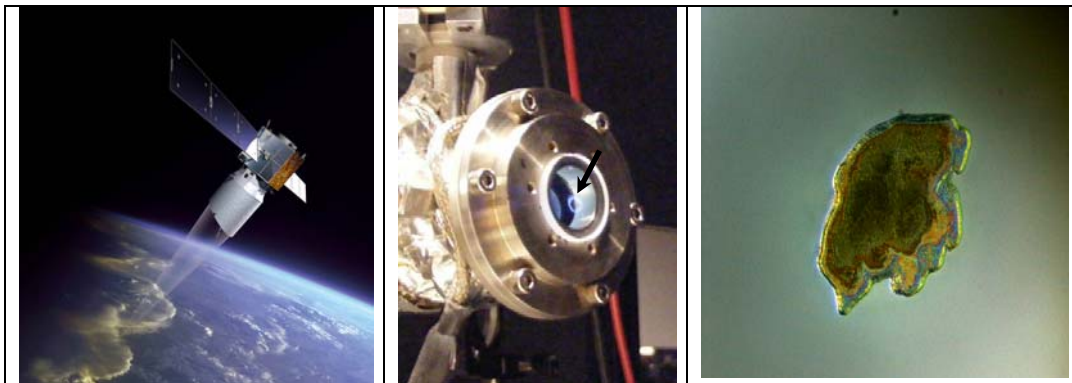


**Figure 1: Aeolus spacecraft (left); Fluorescence of LIC deposit (centre); Damaged optics (right)**

The effect of such phenomenon is critical to the lifetime operation of the laser instrument onboard the spacecraft. The long term optical degradation of each element will contribute to an overall transmission loss and eventual irreversible damage of the optical components. In conclusion, these hazardous effects can compromise the lifetime of missions that carry high-power lasers.

### 3. EXPERIMENTAL SETUP

Figure 2 describes a typical LIC setup with its in-situ monitoring instrumentation.

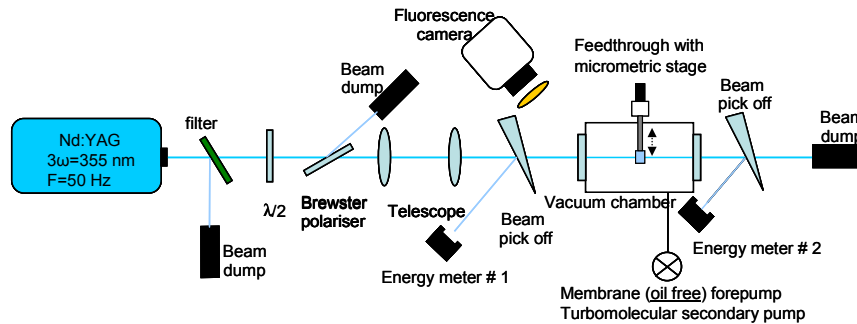


**Figure 2: Typical LIC setup diagram**

The beam from a frequency-tripled Nd:YAG laser (355 nm) is launched through a set of optical components before entering in the test chamber under vacuum. A combination of polarizing components plus a beam expander system is used to adjust the beam diameter in order to match the test fluence required for each LIC test. A set of 2 energy meters at the entrance and exit of the test chamber are used to monitor the relative transmission behaviour during the experiment duration. The sample under test is mounted on a dedicated micrometric stage that is operated from outside the vacuum chamber. To image the fluorescence evolution on the optical component under vacuum a CCD camera is used.

### 4. DETECTION TECHNIQUES

#### 4.1 In-Situ Measurements

##### 4.1.1 Relative transmission

Figure 3 depicts a diagram of the in-situ transmission setup. The instrumentation used to characterize the laser beam transmission through the test chamber is shown.

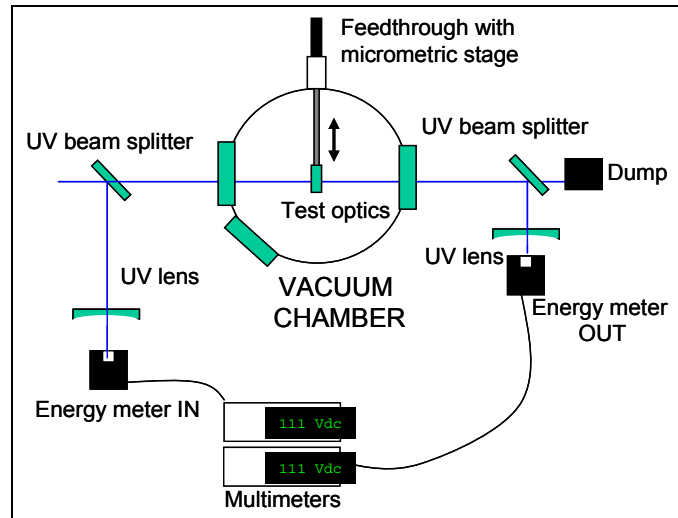


**Figure 3: In-situ transmission setup**

The relative transmission is computed from the measured ratio of the energy transmitted through the chamber (output) and the energy measured in front of the chamber (input). The measurement is performed according to equation (1), by temporarily translating the test optics away from the irradiated area to a different position and measuring the relative change in transmission between the irradiated area (nominal) and the “clean” area (reference). This in-out technique reduces measurement drifts caused by the energy detectors.

$$T = \left[ 1 - \left( \left( \frac{E_{output}}{E_{input}} \right)_{nom} - \left( \frac{E_{output}}{E_{input}} \right)_{ref} \right) \right] \times 100 \quad (1)$$

Additionally, the test optics can be translated out of the beam path to perform an independent measurement.

Figure 4 shows an example of two transmission measurements performed under different environment conditions. The initial test under an environment of 20 Pa of Oxygen pressure (blue line) shows no transmission loss within a few percent (error of the measurement) for approximately 110 Million shots. The second test (red curve) was performed under a lower Oxygen pressure of 5 Pa corresponding to a transmission loss of almost 7 % for approximately 10 Million shots.

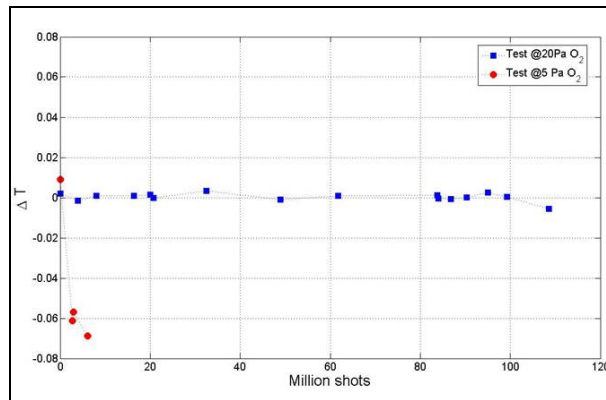


**Figure 4: In-situ transmission measurements ( $T_{loss}$  vs  $T_{no\_loss}$ )**

#### 4.1.2 Fluorescence evolution

The fluorescence evolution is measured during the UV excitation of the deposited material on the optical surfaces under vacuum. This technique allows for the detection of nanometric layers deposited on the optics surface during the test. Figure 5 shows an example of how the fluorescence measurement technique can be implemented.

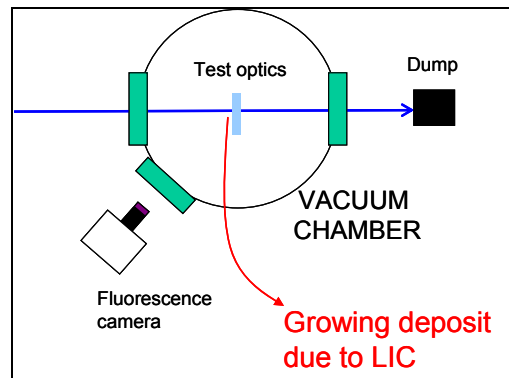


**Figure 5: In-situ fluorescence setup**

The fluorescence signal measured in the visible range of the spectrum is obtained by integration of counts over the laser beam area, resulting in the total number of counts per pixel, according to the following equation (2).

$$F = \frac{\sum_{i,j} (counts)_{i,j}}{N_{pixel}} \quad (2)$$

Figure 6 shows the onset evolution of fluorescence during an LIC test. The fluorescence signal shows an increasing intensity for the total duration of the test. The LIC deposit resembles an annular shape (doughnut) at the end of 65 hours of testing.

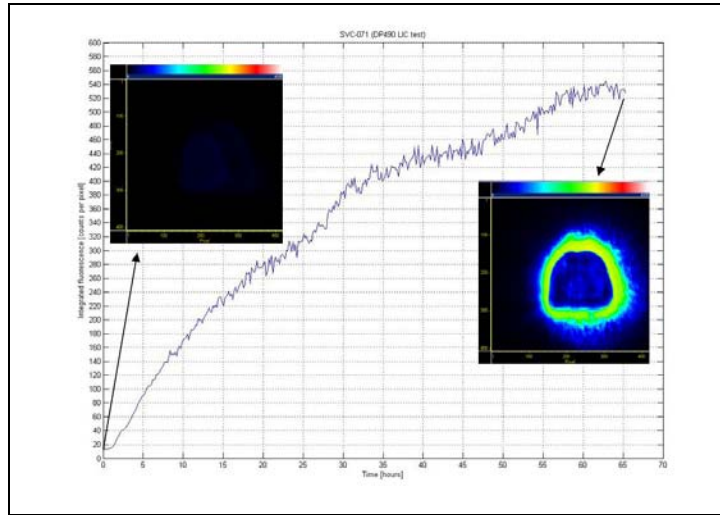


**Figure 6: In-situ fluorescence measurement**

#### 4.2 Ex-situ Analysis

Ex-situ analysis comprises different techniques such as a transmittance/reflectance mapping, fluorescence mapping, white-light interferometry, and optical microscopy (Normarski). Other techniques such as the atomic force microscopy (AFM), mass spectrometry (RGA) and gas chromatography/mass spectrometry (GCMS), and finally chemical analysis such as the time of flight secondary ion mass spectrometry (ToFSIMS) are also used if deemed necessary.

##### 4.2.1 Transmission mapping

The setup developed for mapping the surface of the optical component with respect to transmittance losses is presented in Figure 7. The optical sample under test is illuminated with normal incidence with respect to the surface (in case of transmissive optics) and imaged on a CCD.

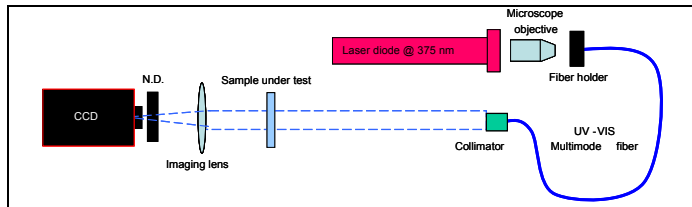


**Figure 7: Ex-situ transmittance setup**

This imaging technique requires a homogenous beam profile distribution. Illuminating the sample surface orthogonally with a flat wavefront ensures a constant intensity over the full diameter of the optic. The setup is validated by measuring a calibration sample with known transmission loss. The transmission image must be referenced to an independent image of the wavefront in free propagation (no optic sample at the beam path); alternatively, a clean new optic (representative of the same coating under the LIC test) can be used as a reference image. In Figure 8, for this particular example we can observe a transmission loss in the order of 6 % on the edge of the deposit.

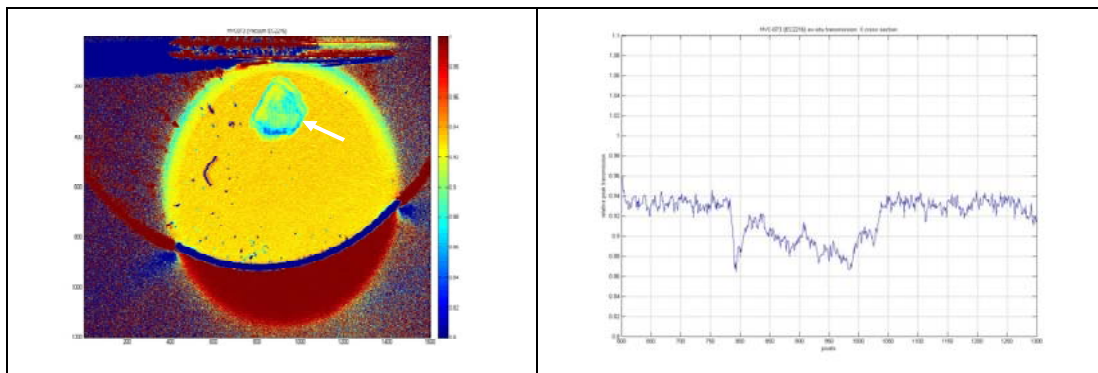


**Figure 8: Ex-situ transmission map (left); and cross section measurement (right)**

In the case of testing reflective optics the setup must be rearranged in a reflective configuration. In this case it is necessary to use an image of the wavefront reflected on a non-irradiated area of the test optics (or representative of the same coating used in the LIC test).

#### 4.2.2 Fluorescence mapping

Figure 9 shows the ex-situ fluorescence measurement setup and an example result. The optical sample under test is illuminated with normal incidence (in case of transmissive optics) and imaged onto a CCD camera.

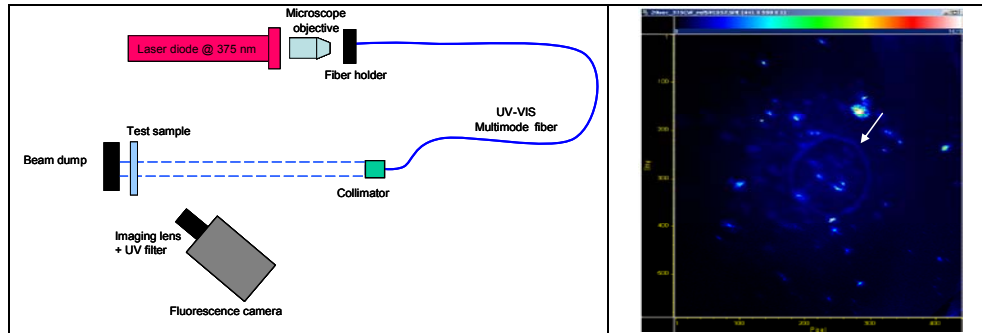


**Figure 9: Ex-situ fluorescence setup (left); example measurement (right)**

This method allows for the measurement of previously deposited layers during an LIC test. Illuminating of the optics surface with UV light produces the visible fluorescence emitted by the LIC deposit. This technique has a detection capability of sub-nanometric layers and is an important tool to measure the formation of a deposit on optics that cannot be accessed during the LIC test.

#### 4.2.3 White-light interferometry

White-light interferometry is a well-known technique that allows for detection and characterization of structures present on the surface of optical components. Figure 10 shows some examples of white-light interferograms performed on optics tested for LIC. We can characterize the deposit shape and topography of such deposits with nanometric resolution.

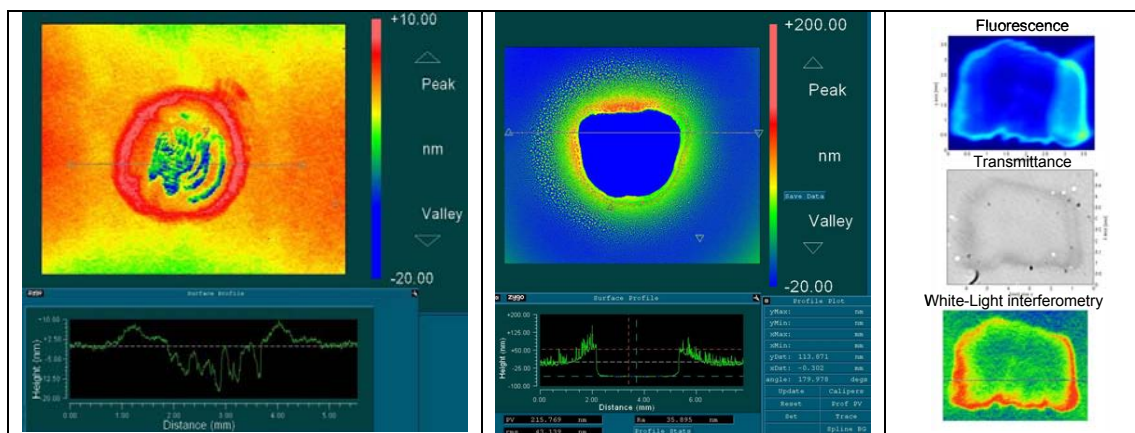


**Figure 10: White-light interferograms (left; centre) and correlation with other techniques (right)**

On the right-hand side picture above it's possible to see that the ex-situ white-light interferogram correlates quite well with the results of the in-situ fluorescence and the ex-situ transmittance techniques.

#### 4.2.4 Optical microscopy

Figure 11 (left-hand side) shows imaging results from the optical microscopy technique. This technique was used to evaluate the presence of a potential laser mark present on the surface of each optic. It's possible to clearly identify the shape and structure of the LIC deposits present on the surface of the optical component under test.

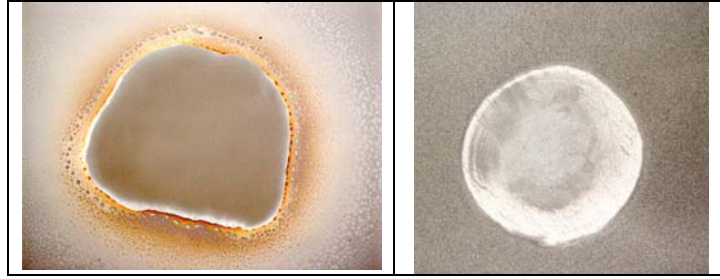


**Figure 11: Optical microscopy of LIC deposits (left); “huff test” (right)**

Figure 11 (right-hand side) shows the result of a technique based on water condensation applied on the surface of the optics (“huff” test). This technique was applied under the microscope in order to increase the contrast of an eventual LIC deposit. This is usually a good indication of the laser beam footprint as the laser is known to increase the hydrophobicity of the optical surface it impinges upon. The process we see is probably dehydroxylation of the fused silica caused by the laser irradiation [4].

This dehydroxylation results in silica surfaces with final-state hydroxyl concentrations similar to those obtained through the thermal treatment of silica above 200°C, indicating that the laser causes a high localized temperature. The modified surface has then significantly increased hydrophobicity compared to the non irradiated silica surface. Based on conclusions from past experiments [5], dehydroxylation is caused by a thermal mechanism and requires sufficient cumulative heating by laser irradiation of the surface. Therefore, more hydroxyls are removed at higher laser fluences and/or repetition rates [4].

## 5. CONCLUSION

LIC detection techniques are available and have nanometric level of resolution. The results from in-situ and ex-situ techniques are well correlated and proven to be efficient in detecting LIC. LIC is a significant risk to the performance of high-powers UV lasers (LIDARS) operating in space, since a large number of optical surfaces will be affected and consequently the overall transmission loss will be critical.

A number of LIC reduction and mitigation techniques [6] [7] can be applied in order to successfully recover the transmission losses observed. Such techniques include a selection of materials and optical coatings; the bake-out of materials as much as possible in order to reduce the outgassing flux of contaminant species; and the shielding of optical components from the contaminants in high conductance. Two novel techniques have been recently developed with efficient results in suppressing the LIC effects: the in-situ LIC cleaning via an Oxygen pressure within the UV optics and the use of molecular absorbers to trap contaminant species nearby.

## 7. ACKNOWLEDGMENTS

The authors acknowledge the valuable contributions from EADS Astrium, Selex Galileo, DLR Stuttgart, Laser Laboratorium Gottingen, Laser Zentrum Hannover, CEA, Institute Fresnel Marseille, and, not least to the team of engineers at ESA ESTEC who have provided interdisciplinary discussions on this challenging phenomenon.

## 8. REFERENCES

- [1] F. Hovis, B. Shepherd, C. Radcliffe, H. Maliborski: “*Mechanisms of contamination Induced Optical Damage in Lasers*”, SPIE Vol. 2428, 1995.
- [2] W. Riede, P. Allenspacher, H. Shroeder, D. Wernham, Y. Lien: “*Laser-Induced hydrocarbon contamination in vacuum*”, SPIE Vol 2714, 2005.
- [3] S. Becker, A. Pereira, P. Bouchout, F. Geffraye, C. Anglade: “*Laser-Induced Contamination of Silica Coatings in Vacuum*”, SPIE Vol 6403, 2007.
- [4] D.M. Kane: “*Glass/UV Laser surface interactions*”, Department of Physics, Macquarie University Sydney, NSW 2009, Australia.
- [5] A.J. Fernandes, D.M. Kane et al. - “*UV Laser-Induced Dehydroxylation of UV Fused Silica Surfaces*”.
- [6] A. Tighe, F. Pettazzi, J. Alves, D. Wernham: “*Growth mechanisms for laser induced contamination on space optics in vacuum*”, SPIE Laser Damage 2008 Symposium proceedings.
- [7] D. Wernham, J. Alves, F. Pettazzi, A. Tighe: “*Risk Mitigation for Laser-Induced Contamination on the ADM-Aeolus Satellite*”, SPIE Laser Damage 2010 Symposium proceedings.